

Universal Dynamic Fragmentation in D Dimensions

J. A. Åström,¹ F. Ouchterlony,² R. P. Linna,³ and J. Timonen³

¹Centre for Scientific Computing, P.O. Box 405, FIN-02101 Esbo, Finland

²Swedish Blasting Research Centre at LTU, Box 47047, S-10074 Stockholm, Sweden

³Department of Physics, University of Jyväskylä, P.O. Box 35, FIN-40014 Jyväskylä, Finland

(Received 10 November 2003; published 18 June 2004)

A generic model is introduced for brittle fragmentation in D dimensions, and this model is shown to lead to a fragment-size distribution with two distinct components. In the small fragment-size limit a scale-invariant size distribution results from a crack branching-merging process. At larger sizes the distribution becomes exponential as a result of a Poisson process, which introduces a large-scale cutoff. Numerical simulations are used to demonstrate the validity of the distribution for $D = 2$. Data from laboratory-scale experiments and large-scale quarry blastings of granitic gneiss confirm its validity for $D = 3$. In the experiments the nonzero grain size of rock causes deviation from the ideal model distribution in the small-size limit. The size of the cutoff seems to diverge at the minimum energy sufficient for fragmentation to occur, but the scaling exponent is not universal.

DOI: 10.1103/PhysRevLett.92.245506

PACS numbers: 62.20.Mk, 46.50.+a, 61.43.Bn

Fragmentation is a process which appears at all length scales. On a nuclear scale, fission produces fragments that are of the size of atomic nuclei. In the range from micrometers to decameters, grains of fragmented rock are called clay, silt, sand, gravel, stones, or boulders, depending on their size. The Earth's crust is fragmented into tectonic plates, and the relevant length scales are 10^4 – 10^7 m. On an astronomic scale, supernovas are obvious fragmentation events.

Generic models of brittle fragmentation have long been focused on Poisson processes in which more or less uncorrelated flaws are activated in the sense that they turn into propagating cracks under external loading. Smooth cracks of dimension $D - 1$ thus produced are usually assumed to propagate until they meet another crack or a boundary of the specimen of dimension D . Gilvarry [1] derived a fragment-size distribution under these assumptions:

$$dn(Q) = V_0 v^{-1} \exp(-Q) dQ, \quad (1)$$

which was experimentally confirmed in the classic paper by Gilvarry and Bergstrom [2]. In Eq. (1) the term $\exp(-Q)dQ$ is the probability of forming a fragment of size v , surface area s , and edge length l , within an interval dQ with $Q = \gamma_l l + \gamma_s s + \gamma_v v$, where the γ 's are the densities of "line," "area," and "volume" flaws, respectively. The line term should here be the dominant one, which means that $dn(Q)$ is reduced to

$$dn(v) = V_0 v^{-[(2D-1)/D]} \exp(-\gamma_l l) dv. \quad (2)$$

The term $V_0 v^{-1}$ in Eq. (1) is the *a priori* number of fragments in dQ . For a Poisson-process fragmentation this term is doubtful as demonstrated by Grady and Kipp [3] by numerical simulations. For $2D$ fragmentation they showed that the *a priori* number of fragments is independent of v , and hence the fragment-size distribu-

tion should be purely exponential. Despite this fact, Eq. (2) has been experimentally confirmed in numerous cases.

In this Letter, we demonstrate that the Gilvarry result can indeed be derived from a Poisson process if one takes into account that propagating cracks become unstable and give rise to side branches that can merge to form additional (small) fragments. Yoffe [4] already pointed out that, above a critical velocity, the stress field around a crack tip develops stress maxima at an angle of ca. 60° on both sides of the tip. It has indeed been demonstrated experimentally [5], numerically [6,7], and theoretically [6,8], that fast moving cracks split. Splitting changes the stress field, but it is soon recovered, and a new splitting takes place. This causes side branches around a crack to appear at intervals with a well-defined mean value [9]. Side branches do not typically have energy enough for further splitting.

Cracks are known to attract each other in the sense that stress intensity in a thin strip of width ϵ between two cracks diverges as $1/\epsilon$. The same applies of course to adjacent side branches which therefore tend to eventually merge. In a merging the tip of a side branch hits a free (fracture) surface left behind by its neighboring branch so that a single branch continues to propagate forward from each merging point. Beyond the first mergings of side branches of a main crack we thus have a "second generation" of branches that continue to propagate and attract each other. Thereby the merging process continues with a decimated number of branches in each new "generation," and correspondingly larger fragments created by mergings. There is ample experimental evidence of dynamical branching, see, e.g., Refs. [10] for results for rock relevant for the present work, and there is also numerical evidence of the kind of merging of side branches described above [11–13].

In accordance with Gilvarry, we assume that flaws within a fragile body are activated when external loading

is applied. In a D -dimensional volume the activated flaws form cracks of dimension $D - 1$, which merge to form fragments. The probability of finding a fragment of size v is simply proportional to the probability of not finding an activated flaw within a volume v . Uncorrelated flaws obey Poisson distribution, and we obtain the size distribution [3]

$$dn_1(v) = V_0 \gamma_v \exp(-\gamma_v v) dv \quad (3)$$

for fragments of linear size l and volume $v \propto l^D$.

Notice that we assume there is no macroscopic notch in the fragile body so that the elastic energy loaded in it by the time fragmentation begins is much higher than in typical laboratory experiments on crack propagation [9]. The cracks created will thus propagate very fast and be unstable for side-branch formation. We thus assume that a main crack produces n_b branches with an average mutual distance of l_b . (For simplicity we consider in what follows branches separated by this average distance; a general model with, e.g., a distribution of mutual distances will be reported elsewhere [14].)

As described above, adjacent branches of these n_b “first-generation” branches will eventually merge to form $n_b/2^{D-1}$ fragments of size l_b^D . Mergings of the farther propagating “second-generation” branches will produce $n_b/(4^{D-1})$ fragments of size $(2l_b)^D$, and this merging process continues as a geometric series. This kind of process (as well as the more general process of Ref. [14]) leads to the fragment-size distribution

$$dn_2(v) \propto n_b v^{-(2D-1)/D} dv. \quad (4)$$

Because of elastic relaxation and energy dissipation, the branching-merging process will, however, be limited to a finite range. This can be taken into account by defining a penetration depth λ for the side branches away from a main crack. This means that, for fragments larger than $(\lambda/2)^D$, the distribution $dn_2(v)$ should decay fast. As the actual shape of the cutoff is not important [14] for the final fragment-size distribution, we assume for simplicity an exponential cutoff: $dn_2(v) \exp[-v/(\lambda/2)^D]$.

Our fragmentation scenario can thus be described such that the main cracks created by external loading form fragments (by merging) in a Poisson-process, while their side branches simultaneously form fragments via the above branching-merging process. The resulting fragment-size distribution can be expressed in the form

$$dn(v) \propto n_b v^{-(2D-1)/D} dn_1(v^*) + M_f dn_1(\hat{v}), \quad (5)$$

where $v^* = v/[\gamma_v(\lambda/2)^D]$, and \hat{v} is related to $v = l^D$ through $\hat{v} \propto (l + \lambda)^D$. The second term on the right-hand side is the residual (fragment size reduced by λ) of the Poisson process after the side-branch fragments have been formed. M_f determines the relative normalization of the two parts, and we assume here for simplicity that it is an independent parameter. Notice, however, that this assumption is well motivated in the large λ limit relevant

for this work, while a more careful consideration may be needed for small λ .

At $D = 1$, fragmentation is just a random breaking of line into pieces. In such a process there are no side branches, which means that n_b and λ must be zero. Equation (5) then reduces to $dn(v) \propto dn_1(v)$ as it should. In higher dimensions we concentrate here on heterogeneous brittle materials (such as, e.g., granite) in which dissipation is small, so that the penetration depth of side branches is relatively large (i.e., $\lambda^D \sim 1/\gamma_v$ and $M_f \rightarrow 0$). This case of large λ is different from that of the rather more ductile and homogeneous PMMA [9]. The fragment-size distribution of Eq. (5) becomes now similar to that of Gilvarry, Eq. (2), with the exception that the cutoff is an exponential function of v instead of l .

When the external load is reduced, the density of activated flaws decreases, so that eventually $\gamma_v \rightarrow 0$. We know from numerical simulations for $D = 2$ [13,15–18] and for $D = 3$ [11,12,16], as well as from experiments [19–25], that this limit appears at a nonzero external load, and that then the fragment-size distribution becomes $dn(v) \propto dn_2(v)$. It means that in this limit $\lambda \rightarrow \infty$.

A similar fragment-size distribution is within the mining community known as the Gaudin-Schuhmann distribution [26,27]. It is usually expressed in the form that the total mass of fragments smaller than \bar{l} scales as \bar{l}^γ with $\gamma \approx 1$. From $dn_g(\bar{l}) = \int_0^{\bar{l}} l^D dn_2(l) dl$ we easily find that $dn_g(\bar{l}) \propto \bar{l}$. Fragmentation of crystalline rock seems thus to be related to the large λ limit, as expected.

We now turn to verification of the full fragment-size distribution Eq. (5). For $D = 2$ a numerical model of a fragile membrane can be constructed as a lattice of mass points connected by elastic beams that break if the strain on them exceeds a given threshold [28,29]. This model allows a detailed analysis of fragmentation under external loading. Figure 1(a) shows a snapshot of a membrane at an early stage of fragmentation induced by homogeneous expansion. A crack is initiated at a single spot and its branching is clearly visible. Figure 1(b) shows the final fragment-size distribution (from several simulations) when the externally applied strain was $\sigma = 1.2$. The curve in this figure is a fit by Eq. (5). Figure 1(c) shows the fragment-size distribution for $\sigma \approx 1$, which is the minimal external strain required for fragmentation to occur, and the line is a fit by Eq. (4) (i.e., by dn_2).

For $D = 3$ the best evidence is provided by real experiments. In the experiments, rock in the Bårarp quarry in Sweden was used in large-scale blasting tests [30]. This rock is reddish granitic gneiss with a typical grain size of 3 to 10 mm, a density of 2670 kg/m³, a compressive strength of 225–250 MPa and a tensile strength of 13 MPa. The measured P -wave velocity was 5400–5650 m/s. Seven single-row rounds were blasted in a 10–12 m long and 5 m high bench, with different hole sizes but with a roughly constant specific explosive charge, $q \approx 0.55$ kg per m³ of rock. The explosive energy supplied was then 1.5–1.8 MJ/m³. The hole diameters

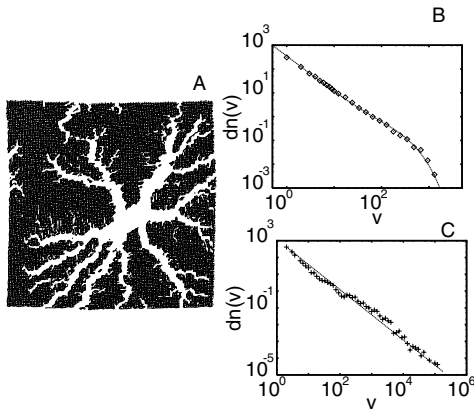


FIG. 1. (a) Snapshot of a small brittle membrane at an early stage of fragmentation (broken bonds are removed so they appear white). (b) The final fragment-size distribution averaged over ~ 30 configurations for $\sigma = 1.2$. The curve is a fit to the data by Eq. (5): $1/\gamma_v = \lambda^D = 22.5$ (in lattice units), and $M_f = 0.007$. (c) Fragment-size distribution in the case of minimal external strain ($\sigma = 1.0$) required for fragmentation. The line is a fit by Eq. (4).

used were 38, 51, 64, and 76 mm. Burden, spacing, and the number of holes per blast were adjusted to the constant specific charge. Before every new blast, a cautious blasting of the bench face was performed in order to reduce the damage zone from the previous blasting, and to create a clean rock surface. Two packaged emulsion explosives were used, Emulite 100 and Kemix from Dyno Nobel with energy contents of 2.7 and 3.2 MJ/kg, respectively. The charges were initiated at 25 ms intervals by electronic programmable delay detonators. All rock in the muck pile except boulders was screened and weighed in three steps. First a Hercules rotary drum sizer was used to obtain five fractions; 0–200, 200–350, 350–400, 400–500, and 500+ mm. The material of the fraction 0–200 mm was then passed through an Extec sizer to obtain four subfractions, 0–25, 25–90, 90–120, and 120–200 mm. Properly quartered samples were taken from the 0–25 mm fraction and sieved in the laboratory. The complete sieving process gave 19 fractions from 0–0.075 to 500+ mm, plus boulders that were counted and weighed separately. The result was thus a fragment-size distribution that covered almost 4 orders of magnitude in linear size or 12 orders of magnitude in mass.

Seven large cylindrical rock samples were also cut from the Bårarp rock and blasted in a closed blasting chamber [31]. The sample diameters chosen were 100, 200, 250, and 300 mm, and the specimens’ height-to-diameter ratios were in the range 1.2–2.1. A single central 5 mm hole was drilled axially. The holes were charged with desensitized PETN powder explosive with an energy content of about 4.17 MJ/kg. The specific charge was thus in the range 0.36–2.9 kg/m³ or 1.5–12 MJ/m³. After blasting, all fragments in the chamber were either picked up or carefully swept together. The coarse 10+ mm material was screened manually in 10 fractions. The

finer material was subjected to a two-step procedure, technical screening with a sieve shaker and subsequent manual screening to guarantee the precision of the technical screening. The loss of material in the blasting was about 0.5–1.5%, and the loss during screening was about 0.05–0.25%. The complete sieving process gave 20 fractions ranging from 0–0.063 to 100+ mm, covering more than 3 orders of magnitude in linear size.

An obvious feature in fragmented rock is that, at a small enough scale, the granular structure of the parent rock affects the fragment-size distribution. It is much harder to fragment single grains than to separate grains from each other. This means that the nonzero grain size introduces an effective small-size cutoff for fragments. If the grain sizes have a continuous distribution $g_r(v)$, we expect that the correction to Eq. (5) can be expressed in the form

$$\hat{d}n(v) = dn(v)[1 + cg_r(v)]dv, \quad (6)$$

where c is the “strength” of the correction. The granular texture of rock is formed by constituents in clastic sediments. The largest grains are composed of chert and polycrystalline quartz. Generically the size distribution of these can be approximated by a log-normal distribution, $g_r(l) \propto \exp[-(\phi(l) - \sigma)^2/w]$, where $\sigma \approx -3$, $w \approx 10$, and $\phi(l) = -\log_2(l)$ is the grain-size parameter used in the so-called Udden-Wentworth scale. Inserting this into Eq. (6), and using parameter c to fit the experimental result, we obtain the results shown in Fig. 2.

It is obvious from Fig. 2(a) that the fragment-size distributions of the quarry experiments are very close to $dn_2(v)$, except for the smallest fragments. This means having $\lambda \rightarrow \infty$ and $\gamma_v = 0$ in Eqs. (5) and (6). The best fit was obtained with $c \approx 14$. The data from the laboratory

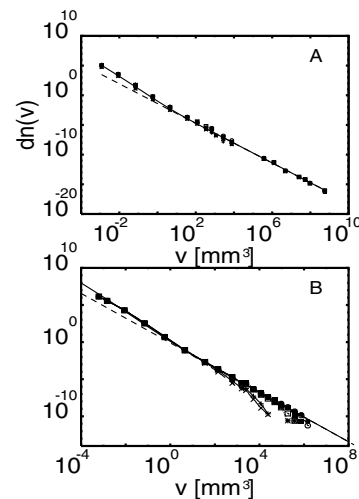


FIG. 2. Experimental fragment-size distributions from quarry blasts (a) and laboratory experiments on cylinders (b). The quarry data are fitted by $dn_2(v)$ (broken line), and by $\hat{d}n_2(v)$ (full line), with $1/\gamma_v$, $\lambda \rightarrow \infty$, and $c = 14.0$. The laboratory data are fitted likewise, except that $c = 2.6$.

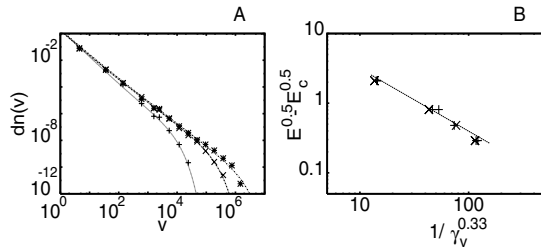


FIG. 3. (a) The large fragment-size part of the data from the laboratory experiments fitted by $dn(v)$, with γ_v as an adjustable parameter. (b) Scaling of the correlation length $\sqrt{1/\gamma_v}$ near the transition point $E = E_c$: $\sqrt{E} - \sqrt{E_c}$ is plotted as a function of $(1/\gamma_v)^{1/3}$, and fitted by a power law with the exponent -0.9 . The resulting correlation-length exponent is $\nu \approx 1.1$.

experiments look very similar except for a cutoff at large sizes. These cutoffs appear at clearly smaller linear fragment sizes than the thicknesses of the cylinders used, and therefore finite-size effects can be ruled out. As expected, the cutoff moves to larger values as the energy input per unit volume (E) is decreased [28]. By estimating the minimum energy input needed to crack the cylinders [$E_c \approx 0.5$ in units of the smallest energy input of the experiments in Fig. 2(b)], the scaling of the cutoff can be investigated. In Fig. 3 we show $(\sqrt{E} - \sqrt{E_c})$ as a function of $(1/\gamma_v)^{1/3}$, and a fit by a power law, which gives -0.9 for the exponent. This means that the correlation-length exponent is $\nu \approx 1.1$. This value should be compared with the correlation-length exponents $\nu \approx 0.67, 3.4, 4.8$ reported in Refs. [18,28]. It is evident that ν is not universal in brittle fragmentation. This lack of universality probably originates from the fact that γ_v is related to the density of activated flaws, which obviously depends on the loading conditions and on the texture of the material.

To summarize, a generic model for brittle fragmentation leads to the fragment-size distribution Eq. (5), and this distribution is in excellent agreement with simulation results in 2D and experimental results in 3D. Further support for this distribution is provided by the very recent experimental results on thin tubes of glass (effectively $D = 2$) [25]. According to this generic model, the fragment-size distribution results from two distinct mechanisms: a crack branching-merging process produces a scale-invariant size distribution in the small fragment-size limit, and a Poisson process produces an exponential cutoff at a system-dependent length scale. This length scale can be interpreted as a correlation length, and it displays nonuniversal scaling behavior. The correlation length, the penetration depth of the branching-merging process, and the mass fraction of the Poisson-process residual, were here used as the free parameters of the model.

- [1] J. J. Gilvarry, *J. Appl. Phys.* **32**, 391 (1961).
- [2] J. J. Gilvarry and B. H. Bergstrom, *J. Appl. Phys.* **32**, 400 (1961).
- [3] D. E. Grady and M. E. Kipp, *J. Appl. Phys.* **58**, 1210 (1985).
- [4] E. H. Yoffe, *Philos. Mag.* **42**, 739 (1951).
- [5] E. Sharon, S. P. Gross, and J. Fineberg, *Phys. Rev. Lett.* **74**, 5096 (1995).
- [6] M. Marder and K. Liu, *Phys. Rev. Lett.* **71**, 2417 (1993).
- [7] J. Åström and J. Timonen, *Phys. Rev. B* **54**, R9585 (1996).
- [8] J. Fineberg and M. Marder, *Phys. Rep.* **313**, 1 (1999).
- [9] E. Sharon and J. Fineberg, *Phys. Rev. B* **54**, 7128 (1996).
- [10] See, e.g., M. Paventi and B. Mohanty, in *Proceedings of FRAGBLAST 7*, edited by X. Wang (Beijing Metall. Ind. Press, Beijing, 2002), pp. 166–172.
- [11] H. Inaoka and H. Takayasu, *Physica (Amsterdam)* **229A**, 5 (1996).
- [12] H. Inaoka, E. Toyosawa, and H. Takayasu, *Phys. Rev. Lett.* **78**, 3455 (1997).
- [13] J. Åström and J. Timonen, *Phys. Rev. Lett.* **78**, 3677 (1997).
- [14] P. Kekäläinen, J. A. Åström, and J. Timonen (to be published).
- [15] J. A. Åström, M. Kellomäki, and J. Timonen, *Phys. Rev. E* **55**, 4757 (1997).
- [16] Y. Hayakawa, *Phys. Rev. B* **53**, 14828 (1996).
- [17] F. Kun and H. J. Herrmann, *Phys. Rev. E* **59**, 2623 (1999).
- [18] J. A. Åström, B. L. Holian, and J. Timonen, *Phys. Rev. Lett.* **84**, 3061 (2000).
- [19] C. J. Waddington and P. S. Freyer, *Phys. Rev. C* **31**, 888 (1985).
- [20] J. E. Finn *et al.*, *Phys. Rev. Lett.* **49**, 1321 (1982).
- [21] T. Kadono and M. Arakawa, *Phys. Rev. E* **65**, 035107 (2002).
- [22] A. Meibom and I. Balslev, *Phys. Rev. Lett.* **76**, 2492 (1996).
- [23] L. Oddershede, P. Dimon, and J. Bohr, *Phys. Rev. Lett.* **71**, 3107 (1993).
- [24] E. S. C. Ching, S. L. Lui, and Ke-Qing Xia, *Physica (Amsterdam)* **287A**, 83 (2000).
- [25] H. Katsuragi, D. Sugino, and H. Honjo, *Phys. Rev. E* **68**, 046105 (2003).
- [26] R. Schuhmann, *Trans. AIME/SME* **217**, 22 (1960).
- [27] A. M. Gaudin and T. P. Meloy, *Trans. AIME/SME* **223**, 40 (1962).
- [28] J. A. Åström, R. P. Linna, and J. Timonen (to be published).
- [29] R. P. Linna, J. A. Åström, and J. Timonen, *Comput. Phys. Commun.* **158**, 26 (2004).
- [30] M. Olsson and I. Bergqvist, in *Proceedings of the Discussion Meeting BK 2002* (Swedish Rock Construction Committee, Stockholm, 2002), pp. 33–38.
- [31] P. Moser, A. Grasedieck, M. Olsson, and F. Ouchterlony, in *Proceedings of the EFEE 2nd World Conference*, edited by R. Holmberg (Balkema, Rotterdam, 2003), p. 449.